Inorganic Chemistry

ARTICLE

pubs.acs.org/IC

Synthesis with Structural and Electronic Characterization of Homoleptic Fe(II)- and Fe(III)-Fluorinated Phenolate Complexes

Stefanie A. Cantalupo,[†] Helen E. Ferreira,[†] Eman Bataineh,[‡] Annie J. King,[‡] Montana V. Petersen,[‡] Teresa Wojtasiewicz,[‡] Antonio G. DiPasquale,[§] Arnold L. Rheingold,[∥] and Linda H. Doerrer*[,†]

[†]Chemistry Department, Boston University, 590 Commonwealth Avenue, Boston, Massachusetts 02215, United States

[‡]Chemistry Department, Barnard College, 3009 Broadway, New York, New York 10027, United States

[§]Department of Chemistry, University of California, Berkeley, 32 Lewis Hall, Berkeley, California 94720-1460, United States

[∥]Department of Chemistry and Biochemistry, University of California, San Diego, 9500 Gilman Drive, La Jolla, California 92093-0358, United States

Supporting Information

ABSTRACT: Four Fe(III) compounds and one Fe(II) compound containing mononuclear, homoleptic, fluorinated phenolate anions of the form $[Fe(OAr)_m]^{n-}$ have been prepared in which $Ar^F = C_6F_5$ and $Ar' = 3,5\text{-}C_6(CF_3)_2H_3$: $(Ph_4P)_2[Fe(OAr^F)_5]$, **1**, $(Me_4N)_2[Fe(OAr^F)_5]$, **2**, $\{K(18\text{-crown-6})\}_2[Fe(OAr^F)_5]$, **3a**, $\{K(18\text{-crown-6})\}_2[Fe(OAr')_5]$, **3b**, and $\{K(18\text{-crown-6})\}_2[Fe(OAr^F)_4]$, **6**. Two dinuclear Fe(III) compounds have also been prepared: $\{K(18\text{-crown-6})\}_2[(OAr^F)_3Fe(\mu_2\text{-}O)Fe(OAr^F)_3]$, **4**, and $\{K(18\text{-crown-6})\}_2[(OAr^F)_3Fe(\mu_2\text{-}OAr^F)_2Fe(OAr^F)_3]$, **5**. These compounds have been characterized with UV−vis spectroscopy, elemental analysis, Evans method susceptibility, and X-ray crystallography. All-electron, geometry-optimized DFT calculations on four $[Ti(IV)(OAr)_4]$ and four $[Fe(III)(OAr)_4]^-$ species (Ar = 2,3,5,6-C_6Me_4H, C_6H_5, 2,4,6-$C_6Cl_3H_2$, C_6F_5) with GGA-BP and hybrid B3LYP basis sets demonstrated that, under D_{2d} symmetry, π donation from the O 2p orbitals is primarily into the d_{xy} and d_{z^2} orbitals. The degree of donation is qualitatively consistent with expectations based on ligand Brønsted basicity and supports the contention that fluorinated phenolate ligands facilitate isolation of nonbridged homoleptic complexes due to their reduced π basicity at oxygen.

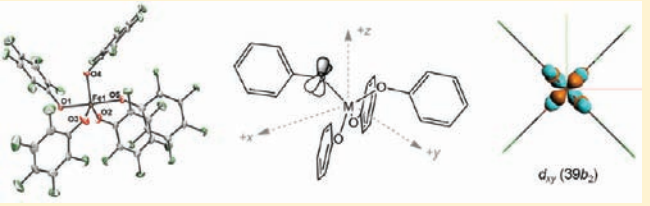

INTRODUCTION

Iron−phenolate coordination is of long-standing interest due to the number of metalloproteins that possess Fe−tyrosine interactions in the active site. Two different forms are common: those enzymes with tyrosine directly bound to the Fe center such as lactoferrins,[1,2] purple acid phosphatases,[3,4] and catechol dioxygenases,[5,6] and those with tyrosine associated with the Fe center in the active site but not directly bound such as ribonucleotide reductase.[7] All of these systems employ Fe and phenolate or phenoxyl groups together to carry out critical biological reactions. Furthermore, metal−aryloxide complexes have been studied as metal−oxide precursors[8,9] and as ancillary ligands in catalysis with virtually every metal in the periodic table.[10−12]

In spite of this tremendous interest in and importance of Fe−phenolate and Fe−tyrosine[13−15] linkages, progress has been slow in preparing simple $[Fe(OAr)_m]^{n-}$ species. Homoleptic, mononuclear alkoxide and aryloxide species are quite rare due to the propensity of the oxygen donor atoms to bridge two or more metal centers.[16] Bulky ortho substituents can prevent bridging as demonstrated[17] with the tetrahedral Fe(III) complexes $(Et_4N)[Fe(OC_6Me_4H)_4]$ and $(Ph_4P)[Fe(OC_6Cl_3H_2)_4]$, the first examples of $[Fe(OAr)_m]^{n-}$ anions.

Recently it was demonstrated that extensive fluorination of aryloxide rings or their substituents is a viable alternative approach that led to facile synthesis and isolation in good yield of homoleptic Co(II),[18] Ni(II),[19] and Cu(II)[18,20] phenolate anions of the form $[M(OAr)_4]^{2-}$. The same approach led to preparation of unusual three-coordinate $[M(OC_4F_9)_3]^-$ compounds with M = Fe(II), Co(II), and Cu(II).[21] Other examples of complexes with fluorinated aryloxide ligands have been shown with coordinatively saturated compounds of Al(III),[22,23] Nb(V),[22,23] and Ta(V)[22,23] as weakly coordinating anions in olefin polymerization catalysis. The fluorination provides an electron-withdrawing environment on the aryloxide ring which pulls electron density away from the O atom. This decreased electron density at oxygen reduces the propensity of ligand bridging without the addition of bulky ortho substituents to the ligand. Analogous nonfluorinated ligands with ortho hydrogen atoms were shown to give dimeric structures in the Co(II) and Cu(II) cases.[18] The extensive ligand fluorination enables the synthesis of mononuclear, homoleptic complexes with a variety of weakly coordinating cations such as {K(18-crown-6)} or

Received: February 22, 2011
Published: June 21, 2011

ammonium/phosphonium R_4E derivatives, as well as coordinating Tl analogs.[18,20]

With Fe however there are no examples of homoleptic $\{Fe(OC_6H_5)_m\}^{n-}$ complexes in the literature. A search of the Cambridge Structural Database for complexes with $Fe-OC_6H_5$ coordination revealed only 17 complexes.[24] The majority of the compounds are multinuclear with bridging aryloxide ligands[25−30] or show terminal $Fe-OC_6H_5$ coordination because the Fe center is bound in a tetraazamacrocycle.[31−34] There are three examples of terminal $Fe-OC_6H_5$ coordination with a terminal NO group bound as well.[35] Herein, we report the extension of the fluorinated ligand approach to the synthesis of homoleptic Fe(II) and Fe(III) phenolate complexes and their structural, electronic, and magnetic characterization.

EXPERIMENTAL SECTION

General Information. All experimental procedures were carried out on a Schlenk line or in a drybox under an atmosphere of purified N_2 at room temperature. The anhydrous solvents tetrahydrofuran (THF), dichloromethane (CH_2Cl_2), diethyl ether (Et_2O), toluene, and hexanes were dried in an alumina-based solvent purification system (SPS) under Ar and piped directly into an MBraun drybox and stored over molecular sieves. Fluorobenzene (FPh) was refluxed over and distilled from CaH_2 and stored over sieves in a N_2-filled drybox. Deuterated solvents used for NMR samples ($CDCl_3$ and CD_2Cl_2) were dried by refluxing over and distillation from CaH_2 and stored over sieves in a N_2-filled drybox. Molecular sieves were used to dry d_6-acetone, which was stored in a N_2-filled drybox. Celite was heated to 125 °C under vacuum overnight. 18-crown-6 was obtained commercially and recrystallized from toluene and hexanes. $KOAr^F$,[18] KOAr′,[18] and $Tl_2(OAr^F)_2\cdot THF$[18] were prepared according to previously published procedures. All other reagents were obtained commercially and used without any further purification. UV−vis data were collected with Varian Cary 50 and Shimadzu UV-3600 spectrometers. NMR spectra were measured on Varian 300 MHz and Bruker Avance 300 MHz NMR spectrometers. NMR spectra were recorded in parts per million (δ), and ^1H chemical shifts were referenced to the resonance of residual protiosolvent. Solution-phase magnetic susceptibilities were determined via the Evans method in d_6-acetone or CD_2Cl_2 with 0.01% $(Me_3Si)_2O$ with the same solution as an internal reference and reported after appropriate diamagnetic corrections.[36,37] Microanalyses were performed by H. Kolbe Microanalytisches Laboratorium, Mülheim an der Ruhr, Germany, and Quantitative Technologies, Inc., Whitehouse, NJ.

Syntheses. *$(Ph_4P)_2[Fe(OAr^F)_5]$*, ***1***. A portion of $FeBr_3$ (79.7 mg, 0.270 mmol) was combined with $KOAr^F$ (300.3 mg, 1.352 mmol) and dissolved in 10 mL of THF to form a dark red-brown solution that was left to stir overnight. The mixture was filtered through Celite to remove KBr, and the filtrate was concentrated to a red oil under vacuum. The oil was triturated three times with CH_2Cl_2 leaving a red-orange powder. A 2 equiv portion of Ph_4PBr (226.7 mg, 0.541 mmol) was added in CH_2Cl_2 and the red-brown solution was left to stir overnight. The reaction mixture was then filtered through Celite to remove KBr and concentrated under vacuum, and the product was recrystallized from CH_2Cl_2 and hexanes at low temperature. Red-brown crystals were isolated in 75% yield (334.9 mg) with one molecule of toluene in the lattice. UV−vis (CH_2Cl_2) (λ_{max}, nm (ε, cm^{-1} M^{-1})): 269 (26 200), 276 (23 100), 312 (11 100), 410 (8460). Anal. Calcd for $C_{78}H_{40}FeP_2F_{25}O_5\cdot C_7H_8$: C, 58.60; H, 2.78. Found: C, 58.46; H, 2.77. μ_{eff} (Evans method, d_6-acetone) = 5.88 μ_B.

$(Me_4N)_2[Fe(OAr^F)_5]$, ***2***. A portion of $Tl_2OAr^F{}_2\cdot THF$ (250.0 mg, 0.645 mmol) was dissolved in toluene to form a clear and colorless solution. $FeBr_3$ (38.1 mg, 0.129 mmol) was added, and the reaction mixture gradually changed to dark red-brown with pale brown precipitate and was left to stir overnight. The reaction mixture was filtered through Celite to remove presumed TlBr, and the red-brown filtrate was concentrated to an oily solid under vacuum. The product was triturated four times with CH_2Cl_2 causing a lighter brown, sticky solid to form. A 2 equiv portion of Me_4NI (51.9 mg, 0.258 mmol) was added in CH_2Cl_2, and the light orange solution was left to stir overnight. Yellow precipitate, presumed TlI, was removed by filtration through Celite, and the orange filtrate was dried under vacuum to an orange solid. The product was recrystallized from THF layered with hexanes. Red-orange crystals formed in 86% yield (125.0 mg). UV−vis (THF) (λ_{max}, nm (ε, cm^{-1} M^{-1})): 272 (15 900), 315 s (9100), 387 (5700). Anal. Calcd for $C_{38}H_{24}Fe\ F_{25}O_5N_2$: C, 40.77; H, 2.16; N, 2.50. Found: C, 40.83; H, 2.12; N, 2.43. μ_{eff} (Evans method, d_6-acetone) = 6.74 μ_B.

$\{K(18\text{-crown-}6)\}_2[Fe(OAr^F)_5]$, ***3a***. A portion of $FeBr_3$ (187.3 mg, 0.634 mmol) was combined with $KOAr^F$ (703.9 mg, 3.17 mmol) in 15 mL of THF, forming a dark red solution, and stirred overnight. The cloudy reaction mixture was filtered through Celite to remove KBr, and the filtrate was concentrated to dryness under vacuum. The resultant dark red powder was triturated three times with CH_2Cl_2, yielding a red-orange powder. A 2 equiv portion of 18-crown-6 (335.0 mg, 1.27 mmol) was added in CH_2Cl_2 to give a red-brown mixture that was stirred overnight. The solution was filtered through Celite to remove residual KBr, and the filtrate was concentrated to dryness. The product was recrystallized from CH_2Cl_2 layered with hexanes, yielding dark red crystals in 45% yield (454.5 mg). UV−vis (CH_2Cl_2) (λ_{max}, nm (ε, cm^{-1} M^{-1})): 265 (19 100), 312 (11 300), 411 (8190). Anal. Calcd for $C_{54}H_{48}FeK_2F_{25}O_{17}$: C, 41.10; H, 3.07; F, 30.10. Found: C, 41.24; H, 3.02; F, 29.88. μ_{eff} (Evans method, $CDCl_3$) = 6.05 μ_B.

$\{K(18\text{-crown-}6)\}_2[Fe(OAr')_5]$, ***3b***. A portion of $FeBr_3$ (72.3 mg, 0.245 mmol) and 5 equiv of KOAr′ (327.4 mg, 1.221 mmol) were combined in 15 mL of THF and stirred overnight. The dark red solution was filtered through Celite to remove KBr, and the filtrate was concentrated to dryness under vacuum. The resultant dark red solid was triturated twice with hexanes, yielding a dark red powder, and three times with CH_2Cl_2, yielding a light red powder. A 2 equiv portion of 18-crown-6 (129.9 mg, 0.491 mmol) was added with 10 mL of CH_2Cl_2, forming a dark red solution that was stirred overnight. The solution was filtered through Celite and then concentrated to dryness under vacuum. The product was recrystallized from CH_2Cl_2 and layered with hexanes to give dark red crystals in 24% yield (105.6 mg). UV−vis (CH_2Cl_2) (λ_{max}, nm (ε_M, cm^{-1} M^{-1})): 244 (22 400), 261 (25 000), 388 (8560). Anal. Calcd for $C_{64}H_{63}FeK_2F_{30}O_{17}$: C, 42.51; H, 3.51. Found: C, 42.46; H, 3.54. μ_{eff} (Evans method, $CDCl_3$) = 6.18 μ_B.

$\{K(18\text{-crown-}6)\}_2[(OAr^F)_3Fe(\mu_2\text{-}O)Fe(OAr^F)_3]$, ***4***. Compound **4** was characterized from a crystal formed by the following reaction: $FeBr_3$ (140.5 mg, 0.475 mmol) was reacted with 5 equiv of $KOAr^F$ (527.9 mg, 2.377 mmol) in 10 mL of THF, forming a dark red brown solution with yellow precipitate. The reaction mixture was filtered through Celite, concentrated to a dark red-brown solid, and triturated three times with CH_2Cl_2. A 2 equiv portion of 18-crown-6 was added, and the solution became less cloudy and was left to stir overnight. The product was recrystallized from CH_2Cl_2 and toluene to form pale red crystals which became orange upon drying. UV−vis (CH_2Cl_2) (λ_{max}, nm (ε, cm^{-1} M^{-1})): 260 (20 200), 313 (11 600), 398 (8190). μ_{eff} (Evans method, CD_2Cl_2) = 4.77 μ_B, per Fe.

$\{K(18\text{-crown-}6)\}_2[(OAr^F)_3Fe(\mu_2\text{-}OAr^F)_2Fe(OAr^F)_3]$, ***5***. A portion of $FeBr_3$ (99.7 mg, 0.337 mmol) was combined with 4 equiv of $KOAr^F$ (299.6 mg, 1.349 mmol) in 15 mL of THF to form a cloudy dark red-brown solution. The reaction mixture was left to stir overnight. The solution was filtered through Celite to remove KBr, and the filtrate was concentrated to dryness under vacuum. CH_2Cl_2 was added, and the product was triturated three times. A 2 equiv portion of 18-crown-6 (178.4 mg, 0.675 mmol) was added in CH_2Cl_2, and the solution was left to stir

dx.doi.org/10.1021/ic2003782 |Inorg. Chem. 2011, 50, 6584–6596

Scheme 1. Syntheses of Homoleptic Iron(III) Aryloxide Compounds 1−3b and 5 and Proposed Formation of μ_2-O-Bridged Fe(III) Dimer 4

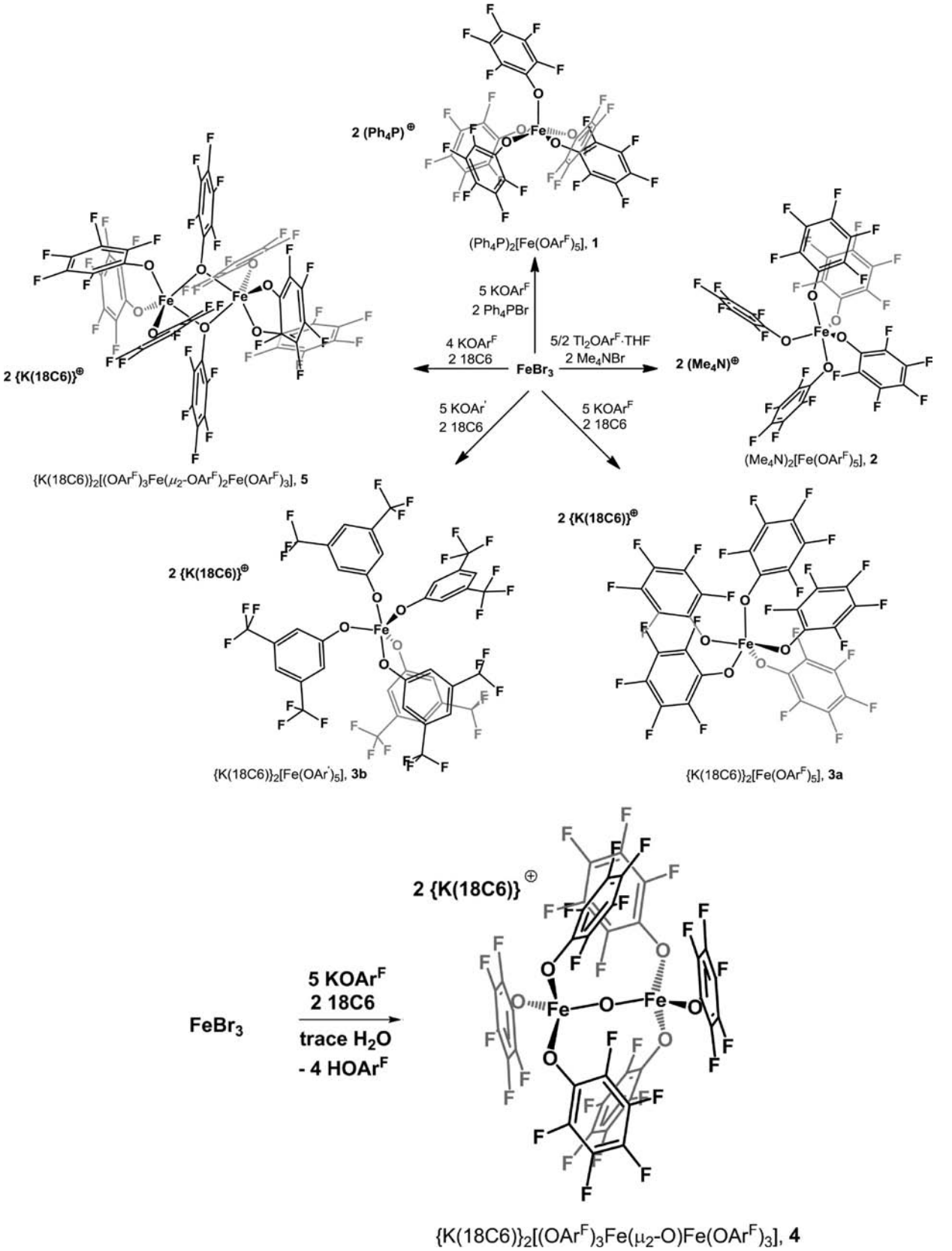

dx.doi.org/10.1021/ic2003782 |*Inorg. Chem.* 2011, 50, 6584–6596

overnight. The solution was filtered through Celite, and the filtrate was concentrated under vacuum. Dark red-brown crystalline material formed by recrystallization in CH_2Cl_2 layered with hexanes at low temperature in 68% yield (252.0 mg). UV−vis (CH_2Cl_2) (λ_{max}, nm (ε, $cm^{-1}\,M^{-1}$)): 260 (29 200), 314 (18 300), 407 (14 700). Anal. Calcd for $C_{72}H_{48}Fe_2K_2F_{40}O_{20}$: C, 39.61; H, 2.22; F, 34.81. Found: C, 39.53; H, 2.03; F, 34.76. μ_{eff} (Evans method, CD_2Cl_2) = 4.15 μ_B, per Fe.

{K(18-crown-6)}$_2$[Fe(OAr^F)$_4$], ***6***. A portion of FeI_2 (92.8 mg, 0.299 mmol) was combined with $KOAr^F$ (267.3 mg, 1.203 mmol) and dissolved in 15 mL of THF, forming a dark yellow-brown solution with a white precipitate that was left to stir overnight. The cloudy reaction mixture was filtered through Celite to remove KI, and the filtrate was concentrated to dryness under vacuum. The dark yellow-brown solid was triturated three times with FPh, forming an off-white/tan-colored powder. A 2 equiv portion of 18-crown-6 (158.9 mg, 0.601 mmol) was added in Et_2O to form a dark yellow-brown mixture that was left to stir overnight. The solution was then filtered through Celite to remove residual KI, and the filtrate was concentrated to dryness. The product was dissolved in Et_2O and layered with hexanes, yielding yellow crystals in 45% yield (186.7 mg). UV−vis (Et_2O) (λ_{max}, nm (ε, $cm^{-1}\,M^{-1}$)): 242 (16 600), 265 (7200), 280 (5900), 320 (2300), 378 (1100). Anal. Calcd for $C_{48}H_{48}FeK_2F_{20}O_{16}$: C, 41.33; H, 3.47; F, 27.24. Found: C, 41.26; H, 3.33; F, 27.04. μ_{eff} (Evans method, d_6-acetone) = 5.40 μ_B.

X-ray Crystallography. All data were collected on APEX-CCD-detector equipped Bruker diffractometers with Mo Kα radiation (λ = 0.71073 Å) and corrected for absorption using semiempirical, multiscan methods. All structures were solved by heavy-atom methods, and the remaining non-hydrogen atoms were located from subsequent difference maps. All structures were refined with anisotropic thermal parameters for all non-hydrogen atoms; hydrogen atoms were treated as idealized contributions. The refinement of F^2 was calculated against ALL reflections. The weighted *R* factor *wR* and goodness of fit *S* are based on F^2; conventional *R* factors *R* are based on *F*, with *F* set to zero for negative F^2. The threshold expression of $F^2 > 2\theta\,(F^2)$ is used only for calculating *R* factors and is not relevant to the choice of reflections for refinement. *R* factors based on F^2 are statistically about twice as large as those based on *F*, and *R* factors based on all data will be even larger. All esds (except the esd in the dihedral angle between two l.s. planes) are estimated using the full covariance matrix. The cell esds are taken into account individually in the estimation of esds in distances, angles, and torsion angles; correlations between esds in cell parameters are only used when they are defined by crystal symmetry. An approximate (isotropic) treatment of cell esds is used for estimating esds involving l.s. planes. The SQUEEZE program was used to account for two hexanes molecules in **3b** based on a void of 492 Å^3, with 108 electrons, which was assigned to two hexane molecules (100 electrons), and the chemical formula unit card was adjusted to account for the change in mass, density, and F_{000} value and to render two unresolved half molecules of toluene in **4**. Due to high disorder, the H atoms in the crown ether of **5** were not included in the final refinement. Data collected at lower temperatures show less pronounced libration in the OAr^F ligands, i.e., **1** (213 K) versus **2** (100 K). All software is contained in various libraries (SHELXTL, SMART, and SAINT) maintained by Bruker AXS, Madison, WI.[38]

RESULTS AND DISCUSSION

The fluorinated ligands, OAr^F and OAr′, chosen for these complexes have been previously characterized in numerous examples[18−20] to form monomeric, homoleptic complexes with late first-row transition metals. In the work reported here, as in our previous studies,[18−20] no significant structural or spectroscopic differences are observed between these two ligands, although both were investigated because variations in crystallinity have been observed.

Scheme 2. Synthesis of Homoleptic Iron(II) Aryloxide Compound 6

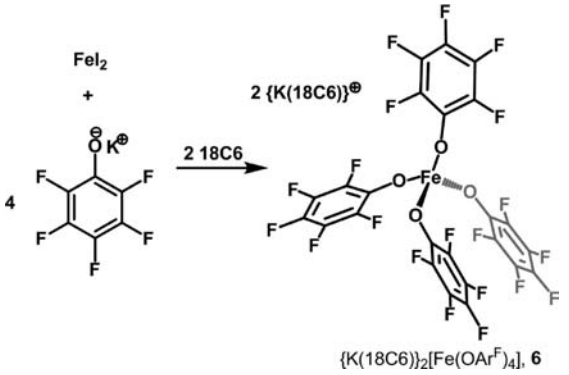

Syntheses. The Fe(III) compounds reported herein, $(Ph_4P)_2$-$[Fe(OAr^F)_5]$, **1**, $(Me_4N)_2[Fe(OAr^F)_5]$, **2**, $\{K(18\text{-crown-}6)\}_2$-$[Fe(OAr^F)_5]$, **3a**, $\{K(18\text{-crown-}6)\}_2[Fe(OAr')_5]$, **3b**, and $\{K(18\text{-crown-}6)\}_2[(OAr^F)_3Fe(\mu_2\text{-}OAr^F)_2Fe(OAr^F)_3]$, **5**, were prepared by simple metathesis reactions as shown in Scheme 1. The potassium or thallium aryloxide salts were reacted with 1/5 equiv of $FeBr_3$ (compounds **1**−**3b**) and 1/4 equiv of $FeBr_3$ for compound **5** followed by removal of KBr. The addition of 18-crown-6 led to compounds **3a**, **3b**, and **5**. Cation-exchange reactions with Ph_4PBr and Me_4NI and further removal of KX or TlX were carried out to form compounds **1** and **2**, respectively. Cation-exchange reactions with Tl salts result in cleaner metathesis reactions due to the very low solubility of TlI; however, the formation of compound **1** through cation exchange with a K salt was successful. Compound **4**, $\{K(18\text{-crown-}6)\}_2[(OAr^F)_3Fe$-$(\mu_2\text{-}O)Fe(OAr^F)_3]$, was prepared by reacting $FeBr_3$ with 5 equiv of potassium aryloxide, apparently with trace water, shown in Scheme 1. We attribute the formation of this bridging oxo unit to trace water due to the conditions under which the synthesis was carried out. The formation of a μ_2-O-bridged Fe dimer suggests that the adventitious water hydrolyzed two ligands per Fe center to form the $[X_3Fe{-}O{-}FeX_3]^{2-}$ unit which is well known for X = Cl[39] and Br.[40] Attempts to prepare $(Et_4N)_2[Fe_2(\mu_2\text{-}O)(OAr^F)_6]$ via metathesis between $(Et_4N)_2$-$[Fe_2OCl_6]$[39] and $KOAr^F$ led to an oily, red-orange material that could not be made crystalline after extensive recrystallization attempts.

The Fe(II) derivative, $\{K(18\text{-crown-}6)\}_2[Fe(OAr^F)_4]$, **6**, was synthesized by an analogous metathesis reaction as shown in Scheme 2. Reaction of FeI_2 with 4 equiv of potassium aryloxide and 2 equiv of 18-crown-6 with subsequent removal of KI resulted in the formation of compound **6**. The solvent CH_2Cl_2 was avoided in this synthesis due to the possibility of oxidation of Fe(II) to Fe(III). Compound **5** was synthesized via metathesis, vide supra, and oxidation. Reaction of **3a** with PhIO as shown in Scheme 3 also produced compound **5**. The addition of PhIO caused the orange-red solution to turn light orange-brown and form red-brown crystals. Crystallographic characterization of the product revealed two μ_2-OAr^F-bridged ligands connecting two Fe centers. This product suggests the loss of two aryloxyl radicals changing the metal to ligand ratio from 1:5 to 1:4. Due to the oxidation of the ligand, future oxidation studies will focus on the fluorinated iron alkoxide complexes.[21]

dx.doi.org/10.1021/ic2003782 |*Inorg. Chem.* 2011, 50, 6584–6596

Scheme 3. Reaction Forming Dimeric Fe Phenolate Complex

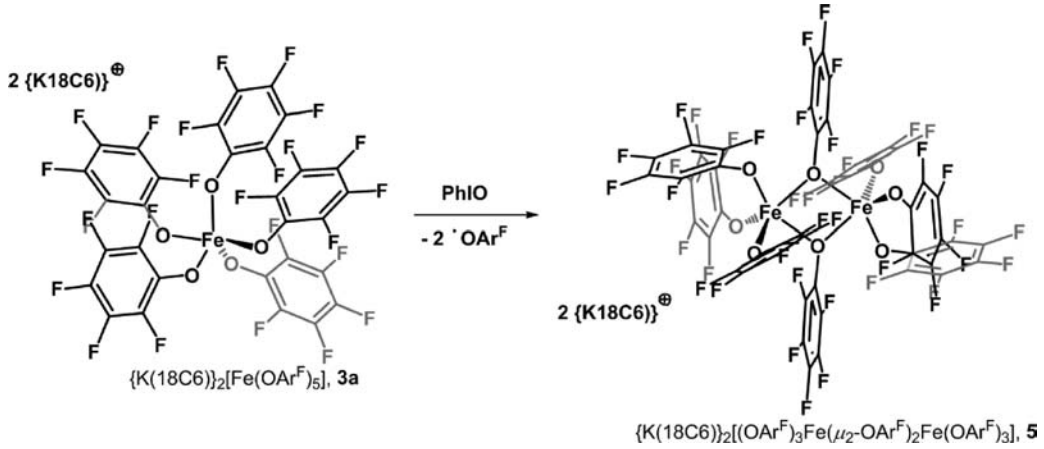

Table 1. Summary of X-ray Crystallographic Data for Fe Aryloxide Complexes

compound	1	2	3a	3b	4	5	6
formula	$C_{85}H_{48}F_{25}FeO_5P_2$	$C_{38}H_{24}F_{25}FeN_2O_5$	$C_{54}H_{48}F_{25}FeK_2O_{17}$	$C_{70}H_{77}F_{30}FeK_2O_{17}$	$C_{67}H_{56}F_{30}Fe_2K_2O_{19}$	$C_{36}H_{24}F_{20}FeKO_{10}$	$C_{52}H_{58}F_{20}FeK_2O_{17}$
fw	1742.02	1119.44	1577.97	1894.37	1924.99	1091.50	1469.03
cryst syst	triclinic	monoclinic	triclinic	triclinic	triclinic	triclinic	monoclinic
space group	*P*-1	*I*2/*a*	*P*-1	*P*-1	*P*-1	*P*-1	$P2_1/n$
a, Å	15.2752(8)	22.466(3)	12.679(8)	14.0618(15)	13.2990(14)	11.4435(8)	14.792(2)
b, Å	15.8820(9)	11.1062(15)	13.338(8)	14.3821(15)	13.3710(14)	14.0079(10)	25.567(4)
c, Å	16.8919(9)	33.506(5)	20.973(13)	21.326(2)	14.0097(14)	14.5871(10)	16.529(2)
α, deg	73.587(1)	90	91.59(1)	88.796(2)	113.9230(10)	97.7070(10)	90
β, deg	68.823(1)	98.504(2)	97.149(11)	74.063(2)	103.6040(10)	110.9000(10)	97.334(2)
γ, deg	88.268(1)	90	114.934(9)	89.938(2)	103.9180(10)	106.8200(10)	90
V, Å^3	3653.5(3)	8268.1(2)	3179(3)	4146.1(8)	2049.0(4)	2016.0(2)	6200.3(15)
Z	2	8	2	2	1	2	4
ρ(calcd), g cm^{-3}	1.584	1.799	1.649	1.517	1.560	1.798	1.574
μ(Mo Kα), mm^{-1}	0.370	0.526	0.508	0.412	0.588	0.627	0.504
temp, K	213	100(2)	208(2)	100(2)	130(2)	100(2)	100(2)
R(*F*), %[a]	5.12	7.49	5.47	8.01	3.49	6.59	8.91
$R(\omega F^2)$, %[b]	13.88	16.23	15.87	25.61	9.30	20.67	25.95

[a] $R = \Sigma||F_o| - |F_c||/\Sigma|F_o|$. [b] $R(\omega F^2) = \{\Sigma[\omega(F_o^2 - F_c^2)^2]\}/\{\Sigma[\omega(F_o^2)^2]\}^{1/2}$; $\omega = 1/[\sigma^2(F_o^2) + (aP)^2 + bP]$ with *a* and *b* given in CIF, $P = [2F_c^2 + \max(F_o,0)]/3$.

Structural Characterization. A search of the Cambridge Structural Database (V5.32)[24] reveals over 1700 examples of Fe with at least five oxygen donor atoms. Within this group, there are 91 examples of Fe complexes bound to *only* five O-donating ligands, excluding water, in which the ligands are primarily carboxylates, carbamates, or alkoxides/phenoxides. Most of the examples reported with this coordination environment are heteroleptic, bridged, or polymeric structures. A rare example of a monomeric Fe complex with five O donor atoms is [calix[4](OMe)$_2$(O)$_2$Fe(THF)].[41] The Fe(II) center is bound by a tetradentate calixarene ligand and one molecule of THF. Prior to this work the only known examples of discrete mononuclear homoleptic phenolate complexes were the $[Fe(OAr)_4]^-$ anions reported[17] with heavily substituted phenoxide groups, $(Et_4N)[Fe(OC_6Me_4H)_4]$ with CH_3 groups in the 2,3,5,6 positions and $(Ph_4P)[Fe(OC_6Cl_3H_2)_4]$ with Cl atoms in the 2,4,6 positions.

Compounds **1**−**6** were crystallographically characterized, and the data collection parameters are summarized in Table 1. Table 2 contains selected interatomic distances and angles for compounds **1**−**6**. The five pentacoordinate complexes have slightly varying geometries at the metal center due to cation/anion interaction and crystal packing forces. The difference in geometry can be quantitatively compared using the five-coordinate geometry index τ_5.[42] The τ_5 parameter is defined by the equation $\tau_5 = (\beta - \alpha)/60$ in which *β* is the largest X−M−X angle and α is the second largest such angle in the coordination sphere. A perfect trigonal bipyramid has $\tau_5 = 1$, and a perfect square pyramid has $\tau_5 = 0$. Similar to the τ_5 parameter, a geometry index for four-coordinate complexes has also been developed,[43] τ_4, defined by the equation $\tau_4 = (360 - (\alpha + \beta))/141$ in which α is the largest angle in the coordination sphere and *β* is the second largest. A perfect tetrahedron has a τ_4 value of 1, whereas a square planar complex has a τ_4 value of 0.

Compound **1** is five coordinate at the Fe center as shown in Figure 1 and has a τ_5 value of 0.07, indicating an almost perfect square pyramid. The aryloxide ligand bound through O2 is in the axial position with an Fe−O_{ax} distance of 1.9085(3) Å. The basal

dx.doi.org/10.1021/ic2003782 |*Inorg. Chem.* 2011, 50, 6584–6596

Table 2. Selected Interatomic Distances (Å) and Angles (deg) for Fe Aryloxide Complexes

	distance (Å)		angle (deg)	
1	Fe1−O1	1.9472(3)	O1−Fe−O2	96.85 (11)
	Fe1−O2	1.9085(3)	O1−Fe−O3	162.61 (11)
	Fe1−O3	1.9324(3)	O1−Fe−O4	88.97 (11)
	Fe1−O4	1.9613(3)	O1−Fe−O5	90.10 (11)
	Fe1−O5	1.9542(3)	O2−Fe−O3	100.54 (11)
			O2−Fe−O4	101.43 (12)
			O2−Fe−O5	100.28 (12)
			O3−Fe−O4	87.60 (10)
			O3−Fe−O5	86.82 (11)
			O4−Fe−O5	158.22 (11)
2	Fe1−O1	1.981(3)	O1−Fe−O2	85.13(14)
	Fe1−O2	1.918(3)	O1−Fe−O3	92.65(15)
	Fe1−O3	1.907(4)	O1−Fe−O4	90.03(14)
	Fe1−O4	1.917(3)	O1−Fe−O5	176.20(14)
	Fe1−O5	1.991(3)	O2−Fe−O3	123.38(16)
			O2−Fe−O4	127.95(16)
			O2−Fe−O5	94.03(14)
			O3−Fe−O4	108.58(16)
			O3−Fe−O5	90.90(15)
			O4−Fe−O5	87.57(14)
3a	Fe1−O1	1.980(3)	O1−Fe−O2	87.64(9)
	Fe1−O2	1.907(2)	O1−Fe−O3	176.5(1)
	Fe1−O3	1.967(3)	O1−Fe−O4	90.7(1)
	Fe1−O4	1.920(2)	O1−Fe−O5	87.5(1)
	Fe1−O5	1.889(2)	O2−Fe−O3	91.5(1)
			O2−Fe−O4	112.6(1)
			O2−Fe−O5	121.6(1)
			O3−Fe−O4	86.5(1)
			O3−Fe−O5	95.8(1)
			O4−Fe−O5	126.0(1)
3b	Fe1−O1	1.984(3)	O1−Fe−O2	83.1(1)
	Fe1−O2	1.915(3)	O1−Fe−O3	91.4(1)
	Fe1−O3	1.911(2)	O1−Fe−O4	173.5(1)
	Fe1−O4	1.987(3)	O1−Fe−O5	93.8(1)
	Fe1−O5	1.917(3)	O2−Fe−O3	131.4(1)
			O2−Fe−O4	92.3(1)
			O2−Fe−O5	124.4(1)
			O3−Fe−O4	88.2(1)
			O3−Fe−O5	104.0(1)
			O4−Fe−O5	92.6(1)
4	Fe1−O1	1.867(1)	O1−Fe−O2	109.58(6)
	Fe1−O2	1.879(2)	O1−Fe−O3	104.82(6)
	Fe1−O3	1.905(1)	O1−Fe−O4	112.26(4)
	Fe1−O4	1.7634(2)	O2−Fe−O3	105.28(6)
			O2−Fe−O4	112.71(5)
			O3−Fe−O4	111.67(4)
5	Fe1−O1	2.048(3)	O1−Fe−O2	93.1(1)
	Fe1−O2	1.917(3)	O1−Fe−O3	150.6(1)
	Fe1−O3	1.897(2)	O1−Fe−O4	95.1(1)
	Fe1−O4	1.867(2)	O2−Fe−O3	94.6(1)
			O2−Fe−O4	98.5(1)
			O3−Fe−O4	111.7(1)
6	Fe1−O1	1.998(3)	O1−Fe−O2	94.1(1)
	Fe1−O2	1.984(4)	O1−Fe−O3	109.0(1)
	Fe1−O3	2.027(3)	O1−Fe−O4	114.4(2)
	Fe1−O4	1.930(5)	O2−Fe−O3	101.6(1)
	K1···O1	2.811(3)	O2−Fe−O4	139.2(2)
	K1···O2	2.858(4)	O3−Fe−O4	96.1(2)
	K2···O3	2.802(3)		
	K2···O4	3.131(5)		

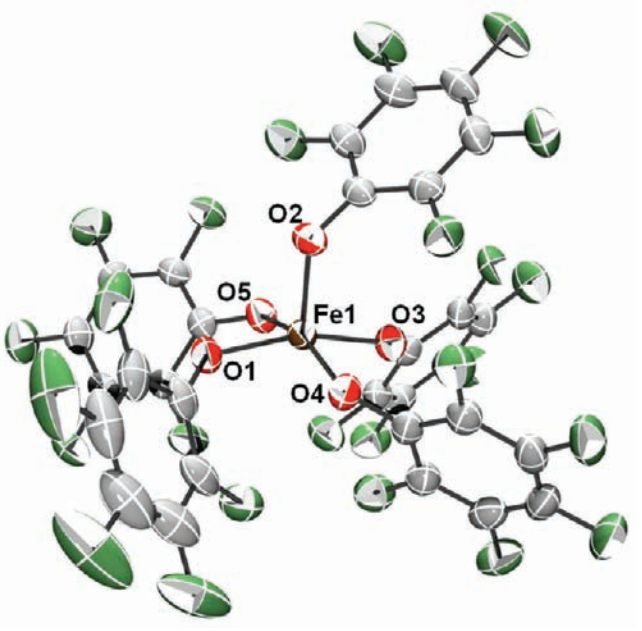

Figure 1. ORTEP diagram of $[Fe(OAr^F)_5]^{2-}$, **1**. The Ph_4P cations and toluene molecule have been removed for clarity. Ellipsoids are shown at the 50% probability level.

Fe−O1 and Fe−O3 distances (1.9472(3) and 1.9324(3) Å, respectively) are slightly shorter than the Fe−O4 and Fe−O5 distances (1.9613(3) and 1.9542(3) Å). The average Fe−O_{basal} bond length with a value of 1.9488(3) Å is considerably longer than the Fe−O_{ax} distance due to mutual trans influences. The basal angles of aryloxides trans to one another are similar at 162.59(9)° and 158.17(9)°. The average O_{ax}−Fe−O_{basal} angle is 99.8(1)° with the Fe atom 0.331 Å above the best O_4 plane. There are $\pi-\pi$-stacking interactions between the phenyl rings on the Ph_4P cation and the aryloxide ligands on the anion. The eight $\pi-\pi$-stacking interactions between the C atoms on the cation and C atoms on the aryloxide rings have an average distance of 3.25(7) Å. The compound crystallized with one molecule of toluene in the lattice. Expanding the unit cell shows no $\pi-\pi$ stacking between the solvent molecule and the anion. The closest C−C contact is at 3.35(1) Å between the toluene methyl C107 atom and C7 on the anion, due to crystal packing effects.

Compound **2** also exhibits a five-coordinate Fe center, but its τ_5 value is 0.80 and is clearly trigonal bipyramidal as shown in Figure 2. The average Fe−O_{ax} bond distance is 1.986(3) Å,

dx.doi.org/10.1021/ic2003782 |*Inorg. Chem.* 2011, 50, 6584–6596

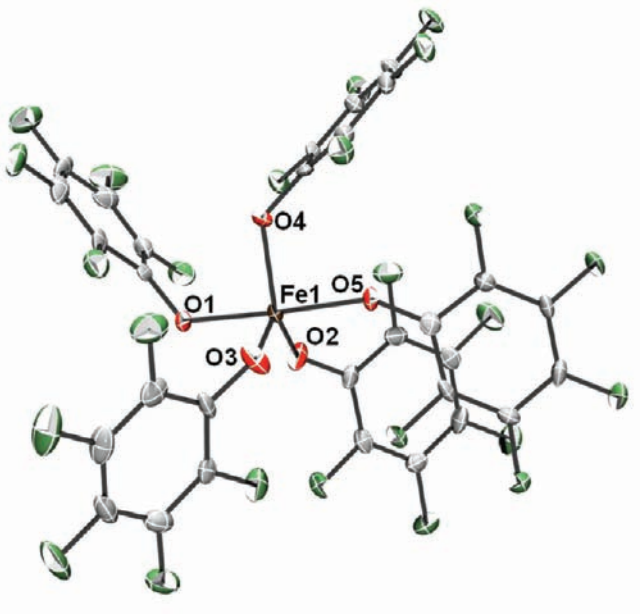

Figure 2. ORTEP diagram of $[Fe(OAr^F)_5]^{2-}$, **2**. The Me_4N cations have been removed for clarity. Ellipsoids are shown at the 50% probability level.

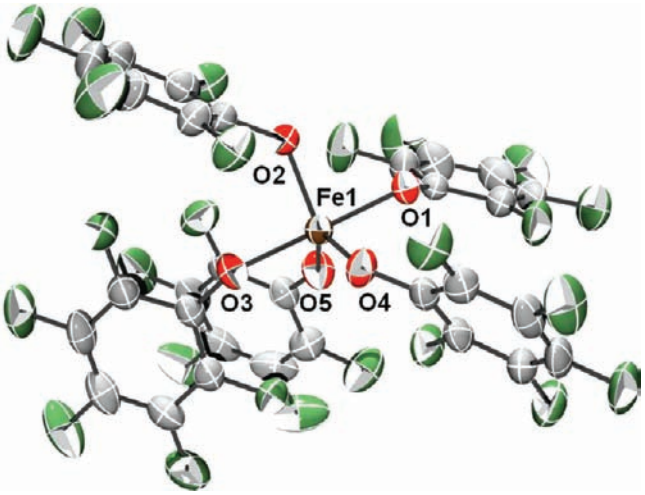

Figure 3. ORTEP diagram of $[Fe(OAr^F)_5]^{2-}$, **3a**. The K(18-crown-6) cations have been removed for clarity. Ellipsoids are shown at the 50% probability level.

which is longer than the average Fe−O_{eq} distance of 1.914(4) Å. The O5−Fe−O1 bond angle is almost linear at 176.2(1)°, and the average O_{eq}−Fe−O_{eq} angle is 120.0(2)°. The average O_{eq}−Fe−O_{ax} angle is 90.1(1) Å. The smaller Me_4N cations in **2** do not participate in any interactions with the anion.

Compound **3a** has a τ_5 value of 0.84 and also has trigonal bipyramidal geometry like that of **2** as seen in Figure 3. The average Fe−O_{ax} bond distance is 1.974(3) Å, which, as expected, is longer than the average Fe−O_{eq} bond distance of 1.905(2) Å. The O_{eq}−Fe−O_{ax} average bond angle is 89.9(1)°, while the axial O−Fe−O angle is nearly linear at 176.5(1)°. Each K atom is encapsulated in a molecule of 18-crown-6 and has longer K···O contacts from aryloxide O atoms at an average distance of

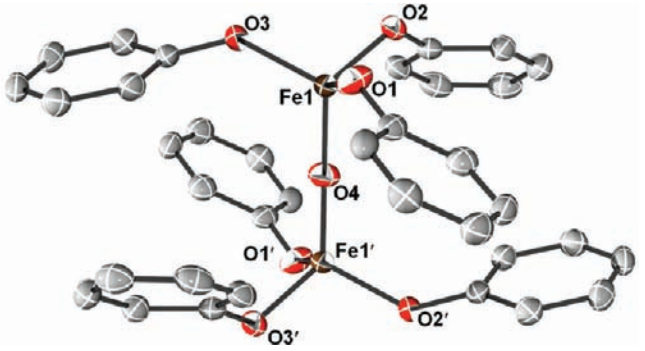

Figure 4. ORTEP of $[(OAr^F)_3Fe(\mu_2\text{-}O)Fe(OAr^F)_3]^{2-}$, **4**. The K(18-crown-6) cations and F atoms have been removed for clarity. Two unresolved half molecules of toluene have also been removed for clarity. Ellipsoids are shown at the 50% probability level.

2.893(3) Å. The anion in **3b** has a trigonal bipyramidal geometry with a τ_5 value of 0.70, as seen in Figure S1, Supporting Information. The structure is very similar to compound **3a** in which the Fe−O_{ax} distances of 1.984(3) and 1.987(2) Å are again longer than the Fe−O_{eq} distances averaging 1.914(3) Å. The bond angles are also similar with a slightly less open axial O−Fe−O angle of 173.5(1)°. The average O_{eq}−Fe−O_{eq} angle is 120.0(1)°. This structure also has interactions between the K cations and the aryloxide O atoms with an average distance of 2.916(3) Å.

Comparison of the square pyramidal geometry in **1** and the approximate trigonal bipyramidal geometry in **2**, **3a**, and **3b** suggests that the trigonal bipyramid is the lowest energy configuration and the $\pi-\pi$ interactions slightly perturb the geometry in **1**. The differences in geometry between **3a** and **3b** are due primarily to the differences in the steric bulk of the ligands. The OAr′ ligand on **3b** has two CF_3 groups in the meta positions unlike the planar OAr^F ligand. This bulk causes the slightly greater distortion from trigonal bipyramidal geometry. The differences in Fe−O bond lengths between these compounds are negligible however. A similar lack of difference was observed in the analogous Co and Cu examples.[18] Therefore, the slightly different pK_a values of the two ligands[44] (OAr^F = 8.42 and OAr′ = 8.26 in trichloroethane) do not have an appreciable effect on the M−O bond lengths.

Compound **4** is a dinuclear structure containing a μ_2-O bridge as seen in Figure 4. The structure has a crystallographic center of inversion at the bridging O atom, imposing a linear Fe−O−Fe angle. The τ_4 value for each Fe is 0.96, indicating a nearly perfect tetrahedral geometry. The distance between each Fe center and the bridging O atom is 1.763(2) Å. There is only one nonhalogen example[45] in the literature with an $X_3Fe-O-FeX_3$ environment similar to compound **4** in which X is a donor from a nonchelating ligand bound to the Fe center. The compound $(Et_4N)_2[(PhS)_3Fe(\mu_2\text{-}O)Fe(SPh)_3]$[45] has three terminal ligands on each Fe center, a τ_4 value of 0.91, indicating a tetrahedral geometry at each Fe center, and a linear Fe−O−Fe angle. The average bond length between each $\{(PhS)_3Fe\}$ unit and the bridging O atom is 1.767(2) Å, which is in good agreement with the data for **4**. The average bond length between the Fe centers and the terminal aryloxide O atoms on **4** is 1.884(2) Å, which is naturally shorter compared to the Fe−S distance of 2.290(4) Å. As seen in the structures for compounds **3a** and **3b**, the K cations in **4** are interacting with two O and two F atoms on the anion.

dx.doi.org/10.1021/ic2003782 |*Inorg. Chem.* 2011, 50, 6584–6596

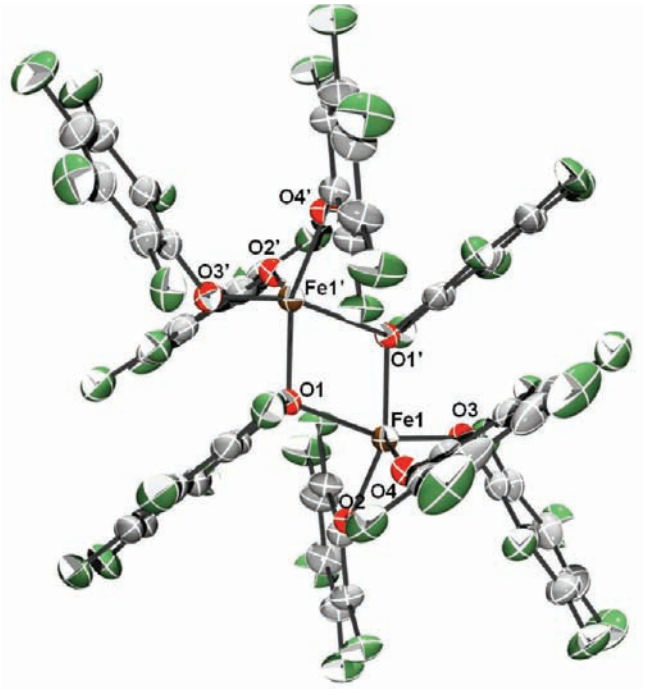

Figure 5. ORTEP of $[(OAr^F)_3Fe(\mu_2\text{-}OAr^F)_2Fe(OAr^F)_3]^{2-}$, **5**. The K(18-crown-6) cations have been removed for clarity. Ellipsoids are shown at the 50% probability level.

The average K···O distance is 2.7913(9) Å, and the average K···F distance is 2.898(3) Å.

Compound **5** has a dimeric structure, consisting of two $\{Fe(OAr^F)_3\}$ units bridged by two μ_2-aryloxides as seen in Figure 5. The τ_5 value for each equivalent Fe center is 0.65, which falls between distorted trigonal bipyramidal and square planar geometry due to the presence of two bridging ligands which constrain the geometry around the Fe center. The average $Fe-O_{bridge}$ distance is 2.032(3) Å with an $O_{bridge}-Fe-O_{bridge}$ angle of 72.0(1)°. The $Fe-O_{terminal}$ distances are an average of 1.893(3) Å, and the Fe···Fe distance is 3.2880(7) Å. This dimer is similar to the previously discussed compounds **3a**, **3b**, and **4** in that the K cations are interacting with F atoms on the anion at an average distance of 3.016(4) Å.

There are fewer still examples of small molecules with an exclusively $\{FeO_4\}$ environment. To date there are over 2500 examples of Fe with at least four oxygen donor atoms but only 51 structurally characterized examples of Fe bound to only four O-donating ligands, excluding water, the majority of which do not have aryloxide ligands. Those that do are the two $[Fe(OAr)_4]^-$ complexes mentioned previously,[17] the Fe(II) coordinated to a bis-alkylated calix[4]arene[46] and a related bis-2,6-isopropylphenyl derivative, $[(THF)_4Na_2Fe(ODIPP)_4]$,[47] which exhibits Na···O coordination to the aryloxide O atoms and has a τ_4 value of 0.34 indicating a geometry much closer to square planar. This substantially greater distortion from tetrahedral geometry is likely due to the shorter Na···O interactions, which have an average distance of 2.27(1) Å, than the related K···O interactions of 2.900(5) Å in **6**, explaining the very different geometries.

Compound **6** is a four-coordinate tetrahedral Fe(II) complex similar to the previously reported compounds $\{K(18C6)\}_2[Co(OAr^F)_4]$[18] and $K\{K(18C6)\}[Ni(OAr^F)_4]$[19] and can be seen in Figure 6. Compound **6** has average Fe−O bond distances of 1.984(6) Å. The τ_4 value for compound **6** is 0.76, indicating a very distorted tetrahedral geometry at the Fe center. The analogous Co and Ni compounds are also distorted tetrahedral structures with τ_4 values of 0.79 and 0.74, respectively. The distortion is due to the {K(18C6)} cation interaction with the anion as discussed for compounds **3a**−**5**. The average K···O distance to the anion in **6** is 2.90(5) Å, and these interactions can be seen in Figure S2, Supporting Information. Notably, the compound $[(THF)_4Na_2Fe(ODIPP)_4]$ is reported to be very sensitive to air and also susceptible to decomposition in a N_2 atmosphere. This behavior is distinct from that of **6**, which is robust in a N_2 environment and shows no signs of decomposition. Thus, **6** is a highly unusual species and the only such Fe(II) tetraaryloxide that we are aware of with neither a chelate ring nor bulky ortho groups.

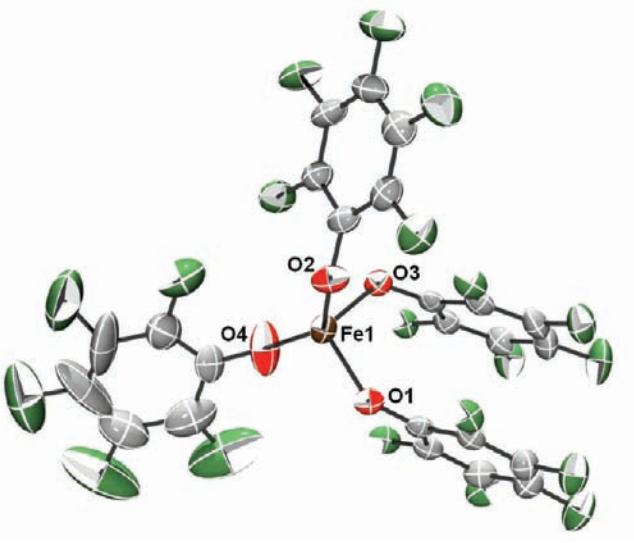

Figure 6. ORTEP of $[Fe(OAr^F)_4]^{2-}$, **6**. The K(18-crown-6) cations and Et_2O molecule have been removed for clarity. Ellipsoids are shown at the 50% probability level.

Magnetism. The Evans method was used to determine solution magnetic susceptibility measurements.[36,37] The four Fe(III) monomeric five-coordinate compounds **1**−**3b** have μ_{eff} values consistent with a spin-only value of 5.9 μ_B. In Fe(II)-containing **6**, the μ_{eff} = 5.40 μ_B, higher than the S = 2 spin-only value of 4.90 μ_B but not unusual for tetrahedral d^6 species. As with previous fluorinated phenolate compounds,[18,19] only high-spin complexes are observed.

Dinuclear **4** has a magnetic moment of 4.77 μ_B per Fe center, which is lower than the expected value for a high-spin S = 5/2 system of 5.9 μ_B. The decrease in μ_{eff} can be attributed to antiferromagnetic coupling between the Fe centers. A recent publication[48] investigated the change in the magnetic moment in the $[Fe_2OCl_6]^{2-}$ dianion as a function of variation in unimolecular dications. The magnetic moments were observed in the range 3.17−4.79 μ_B, like that of compound **4**. The magnetic moment of compound **5** is 4.14 μ_B per Fe, which is also a lower magnetic moment than expected for a high-spin S = 5/2 system due to antiferromagnetic coupling through the OAr^F bridging ligands. Other Fe dimers with bridging OAr ligands such as $[Fe(O(2,4,6\text{-}^tBu_3C_6H_2))_2]_2$[49] and $(Et_4N)_2[Fe_2Cl_4(OC_6H_4\text{-}p\text{-}CH_3)_2]$[50] have magnetic moments of 3.4 μ_B and 4.8 μ_B per Fe

dx.doi.org/10.1021/ic2003782 |Inorg. Chem. 2011, 50, 6584–6596

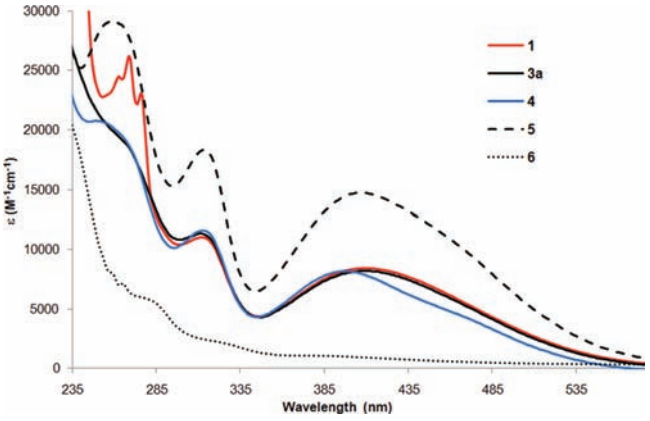

Figure 7. UV−vis spectra (solvent used) of Fe(II) and Fe(III) aryloxide compounds $(Ph_4P)_2[Fe(OAr^F)_5]$ (CH_2Cl_2), **1**, $\{K(18\text{-crown-6})\}_2[Fe(OAr^F)_5]$ (CH_2Cl_2), **3a**, $\{K(18\text{-crown-6})\}_2[(OAr^F)_3Fe(\mu_2\text{-}O)Fe(OAr^F)_3]$ (CH_2Cl_2), **4**, $\{K(18\text{-crown-6})\}_2[(OAr^F)_3Fe(\mu_2\text{-}OAr^F)_2Fe(OAr^F)_3]$ (CH_2Cl_2), **5**, and $\{K(18\text{-crown-6})\}_2[Fe(OAr^F)_4]$ (Et_2O), **6**.

center, respectively, again consistent with the magnetic moment of **5**.

Electronic Spectra. The electronic spectra of compounds **1**, **3a**, **4**, and **5** are very similar to one another as seen in Figure 7. Compounds **1**−**3b** are all dark orange in the solid state. Despite the distinct solid state geometries discussed earlier, the spectra suggest that these compounds have essentially identical electronic environments in solution. The spectra have intense $\pi \rightarrow \pi^*$ absorptions in the UV region with extinction coefficients above 20 000 M^{-1} cm^{-1} and a ligand-to-metal charge transfer absorption around 400 nm in the visible region with extinction coefficients above 8000 M^{-1} cm^{-1}. In the solid state, compound **4** is lighter in color than the monomeric Fe(III) compounds and compound **5**. Compound **6** is pale colored in the solid state and much lighter than compounds **1**−**5**. The electronic spectrum for this compound has two intense peaks at 242 and 265 nm with a less intense absorption at 280 nm. The shoulder at 320 nm and less intense, broad peak centered at 378 nm have much smaller extinction coefficients as shown in Figure 7.

As part of understanding the steric and electronic properties of these new homoleptic species, we sought other homoleptic FeX_5^{2-} or FeX_4^{2-} anions. Such species are exceedingly rare, but the solid state literature records examples of salts containing homoleptic $\{FeX_5\}^{2-}$ groups, such as $A_2FeCl_5\cdot H_2O$[51] (A = NH_4^+, K^+) or $SrFeF_6$[47] that present octahedral Fe(III) atoms in $[FeCl_5(OH_2)]^{2-}$ or edge-sharing $[FeF_6]^{3-}$ octahedra. According to the Cambridge Structural Database (V 5.32),[24] there are only four ordered, structurally characterized examples of the $[FeCl_5]^{n-}$ anion,[52−55] three of which[52−54] are Fe^{III}-containing $[FeCl_5]^{2-}$ and one of which contains Fe^{II} incorporated via μ_2-Cl atoms into a larger $\{Fe^{II}{}_5Cl_8\}^{2+}$ cluster.[55] In the three discrete $[FeCl_5]^{2-}$ anions, the geometry is almost perfectly trigonal bipyramidal, whereas the other example has square-pyramidal geometry enforced by μ_2-bridging carboxylate ligands. To the best of our knowledge there are no other structurally characterized examples of discrete pentacoordinate, halogenated $[FeX_5]^{2-}$ anions. No UV−vis data for the discrete $[FeCl_5]^{2-}$ anion are reported, although the crystals are described as red[52] and dark yellow[53] in the cases of colorless cations. In contrast to the difficulty in isolation of the $[FeCl_5]^{2-}$ anion, the $[Fe(OAr)_5]^{2-}$ species are readily synthesized and purified in good yields.

A search of the Cambridge Structural Database (V 5.32)[24] revealed 94 structurally characterized $[FeX_4]^{2-}$ anions where X is any halogen. The anions have τ_4 values that range from almost perfect tetrahedral geometry at 0.99 to more distorted tetrahedral geometry at 0.74. The τ_4 value for compound **6** is 0.76, which is within the range of the FeX_4^{2-} compounds reported. The distortion in **6** is due to cation interactions with the anion. A qualitative comparison of compound **6** shows strong LMCT in the UV region compared to $FeCl_4^{2-}$ and $FeBr_4^{2-}$.[56]

DFT Calculations. Previously we reported the changes in electronic spectra and ligand field in the $[NiX_4]^{2-}$ systems as a function of the ligand X, which placed the fluorinated alkoxide and aryloxide ligands with medium-field ligands such as OH^- and F^-.[19] Herein, we report a computational study of homoleptic metal phenolate species that elucidates the changes in d-orbital energy as an indicator of LMCT variation with phenolate substituents and more specifically how highly fluorinated character permits isolation of homoleptic phenolates which have not been isolated with nonfluorinated derivatives lacking bulky ortho substituents.

Two different electronic configurations in $[M(OAr)_m]^{n-}$ series were studied to investigate LMCT: closed-shell d^0 in Ti(IV) without d−d transtions and d^5 in Fe(III). Four $[Ti(OAr)_4]$ species and the analogous four $[Fe(III)(OAr)_4]^-$ anions were studied in which OAr = OC_6H_5, OAr^F, OC_6Me_4H, and $OC_6Cl_3H_2$. The latter two phenoxides were chosen because of the availability of structural data for the Fe(III) compounds $(Et_4N)[Fe(2,3,5,6\text{-}OC_6Me_4H)_4]$ and $(Ph_4P)[Fe(2,4,6\text{-}OC_6Cl_3H_2)_4]$.[17] D_{2d} symmetry was used in all cases. All-electron, geometry-optimized calculations were performed with GGA-BP and hybrid B3LYP functionals. Table 3 gives a comparison of interatomic distances and angles between crystallographic (where available) and computational values for the Fe(III) species. Given the artificial imposition of D_{2d} symmetry on all structures, the agreement is reasonable.

On the basis of substituent electron donation character and estimated aqueous pK_a values,[57] the following abbreviated ligand field series was anticipated, with the perfluorinated phenolate being the weakest π donor and the tetramethyl derivative the strongest one.

$$OC_6Me_4H(pK_a = 10.9) > OC_6H_5(9.9) > OC_6Cl_3H_2(6.6)$$

$$> OC_6F_5(5.5)$$

Depicted in Scheme 4 are the qualitative changes in ligand field to be expected with reduction in symmetry from T_d to D_{2d}. In full T_d symmetry, the d_{xz}, d_{yz}, and d_{xy} orbitals are degenerate but with compression along the z axis the $d_{x^2-y^2}$ and d_{xy} orbitals are raised in energy, relative to the d_{z^2} and d_{xz},d_{yz} pair, respectively. The addition of π-basic contributions from oxygen donor ligands should cause further changes, depending on the orientation of the oxygen atom lone pairs. Also present in the scheme is a generic D_{2d} $[M(OAr)_4]$ species with two oxygen lone pairs shown explicitly. The two lone pairs on each oxygen atom are disposed perpendicular to one another such that one is in the aryloxide plane and the second extends above and below that plane. One example of each of the resultant four symmetrically distinct d orbitals from the $[Fe(III)(OAr^F)_4]^-$ B3LYP calculation is shown in Figure 8. The out-of-plane pairs interact with $d_{x^2-y^2}$ (b_1) and d_{xz}/d_{yz} (e_1) orbitals, while the in-plane O lone pairs interact with the d_{z^2} (a_1) and d_{xy} (b_2) orbitals.

dx.doi.org/10.1021/ic2003782 |Inorg. Chem. 2011, 50, 6584–6596

Table 3. Comparison of Interatomic Distances (Å) and Angles (deg) in $[Fe(OAr)_m]^{n-}$ Species[a]

compound	X-ray		DFT	GGA-BP	B3LYP
$(Et_4N)[Fe(2,3,5,6\text{-}OC_6Me_4H)_4]$	Fe(1)−O(1)	1.8264(6)		1.881	187.3
BOFBAZ	Fe(1)−O(2)	1.8596(6)			
	Fe(1)−O(3)	1.8516(6)			
	Fe(1)−O(4)	1.8470(6)			
	O(1)−Fe−O(2)	112.50		111.9 × 4	111.6 × 4
	O(1)−Fe−O(3)	110.77		104.6 × 2	105.3 × 2
	O(1)−Fe−O(4)	108.50			
	O(2)−Fe−O(3)	105.86			
	O(2)−Fe−O(4)	109.57			
	O(3)−Fe−O(4)	109.61			
	Fe(1)−O(1)−C(11)	136.69		155.8	156.1
	Fe(1)−O(2)−C(1)	131.27			
	Fe(1)−O(3)−C(31)	137.18			
	Fe(1)−O(4)−C(21)	142.01			
$[Fe(OPh)_4]^-$			Fe−O	1.891	1.880
			O−Fe−O	113.6 × 4	113.6 × 4
				101.5 × 2	101.6 × 2
			Fe−O−C	137.2	137.5
$(Ph_4P)[Fe(2,4,6\text{-}OC_6Cl_3H_2)_4]$	Fe(1)−O(1)	1.8633(3)	Fe−O	1.890	1.878
BOFBED	Fe(1)−O(2)	1.8668(3)			
	Fe(1)−O(3)	1.8749(3)			
	Fe(1)−O(4)	1.8590(3)			
	O(1)−Fe−O(2)	107.43	O−Fe−O	112.4 × 4	112.1 × 4
	O(1)−Fe−O(3)	105.58		103.8 × 2	104.4 × 2
	O(1)−Fe−O(4)	122.94			
	O(2)−Fe−O(3)	116.29			
	O(2)−Fe−O(4)	99.33			
	O(3)−Fe−O(4)	105.92			
	Fe(1)−O(1)−C(1)	132.15	Fe−O−C	152.2	152.8
	Fe(1)−O(2)−C(7)	133.61			
	Fe(1)−O(3)−C(13)	128.88			
	Fe(1)−O(4)−C(19)	140.79			
$[Fe(OAr^F)_4]^-$			Fe−O	1.892	1.882
			O−Fe−O	110.9 × 4	111.4 × 4
				106.6 × 2	105.7 × 2
			Fe−O−C	142.4	141.4

[a] Numbers in parentheses are estimated deviations of the last significant figure.

The calculations for all four ligands with Ti(IV) and Fe(III) are consistent with the anticipated ligand field such that the three orbitals from the former t_2 set in T_d symmetry are above those of the former e set. The percent O 2p character for the d-based orbitals on Ti(IV) and the β-spin d-based orbitals for Fe(III) are collected in Table 4 and show that the greatest π donation is to the d_{z^2} and d_{xy} orbitals. These changes are reflected in the energy level diagram in Figure 9 in which the energies of the empty d orbitals from the $[Ti(OAr)_4]$ calculations, for four ligands and two different functionals, are displayed from left to right. The analogous energies of the β-spin d-based orbitals for the four Fe(III) compounds are shown in Figure 10. The $d_{x^2-y^2}$ orbital energy level was set to zero energy in all cases, and the other orbital energies are presented relative to that orbital.

The π donation from O 2p orbitals into the metal d_{xy} orbital is expected to be larger for the OC_6Me_4H and OC_6H_5 ligands and is borne out by the data in Table 4. Interestingly, the proportional contribution is largest from the perhydro ligand, rather than the tetramethyl case. Similarly, more π donation, greater O 2p character, is evident in the d_{z^2} orbitals of these two ligands. The $OC_6Cl_3H_2$ and OAr^F ligands are less strongly π donating, and this electronic character is also demonstrated in Table 4, which shows smaller O 2p contributions to the d_{xy} and d_{z^2} orbitals. Consistent with the estimated pK_a values,[57] the

dx.doi.org/10.1021/ic2003782 |Inorg. Chem. 2011, 50, 6584–6596

Scheme 4. Ligand Field Splittings for T_d and D_{2d} Symmetries with a Generic $[M(OAr)_4]^{n-}$ Species in D_{2d} Symmetry Showing Orientation of O 2p Orbitals

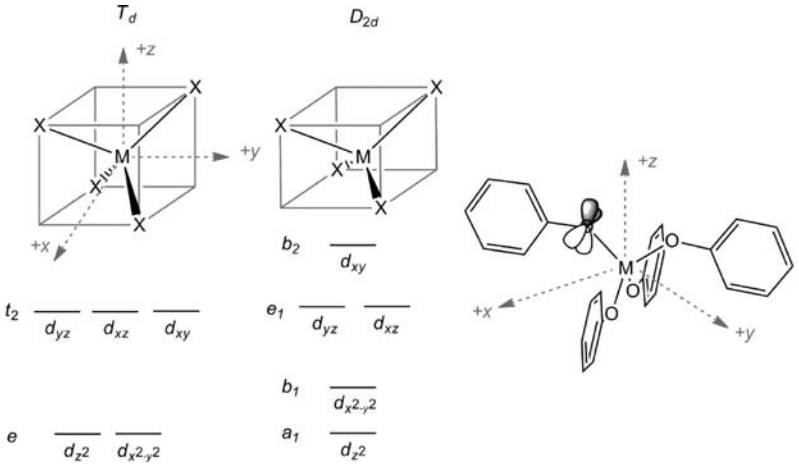

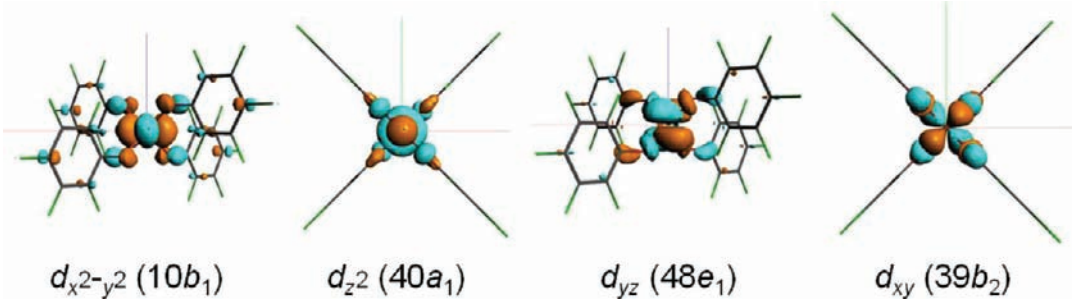

Figure 8. β-spin d-based orbitals from $[Fe(III)(OAr^F)_4]^-$ calculated with the B3LYP hybrid functional, viewed down the y-axis for the $d_{x^2-y^2}$ and d_{yz}, and down the z-axis for the d_{z^2} and d_{xy}. The x axis is shown in red, the y axis in green, and the z axis in blue.

Table 4. Percent Oxygen 2p Character in d-Based Molecular Orbitals

compound	functional	$d_{x^2-y^2}$ (b_1)	d_{z^2} (a_1)	d_{yz}/d_{xz} (e_1, each)	d_{xy} (b_2)
$[Ti(OC_6Me_4H)_4]$	GGA-BP	10.83	15.46	5.35	16.95
	B3LYP	9.75	14.18	5.00	16.40
$[Ti(OC_6H_5)_4]$	GGA-BP	10.59	15.17	4.39	19.07
	B3LYP	9.59	13.62	4.30	18.30
$[Ti(OC_6Cl_3H_2)_4]$	GGA-BP	8.92	14.38	3.47	15.39
	B3LYP	8.22	13.33	3.40	14.68
$[Ti(OAr^F)_4]$	GGA-BP	11.29	13.94	4.08	15.94
	B3LYP	10.13	12.89	4.17	15.26
$[Fe(OC_6Me_4H)_4]^-$	GGA-BP	14.76	16.54	6.59	18.90
	B3LYP	11.27	12.66	5.30	17.37
$[Fe(OC_6H_5)_4]^-$	GGA-BP	14.53	10.72	10.72	21.23
	B3LYP	10.77	8.16	8.07	19.20
$[Fe(OC_6Cl_3H_2)_4]^-$	GGA-BP	12.56	14.62	5.09	17.94
	B3LYP	9.49	11.85	4.06	16.50
$[Fe(OAr^F)_4]^-$	GGA-BP	14.47	11.82	8.34	18.89
	B3LYP	10.96	9.00	6.83	17.40

perfluorinated phenoxide is the least donating among all four ligands. These two trends are most clear in the $[Ti(OAr)_4]$ family, in which the variation in d-orbital energies is not affected

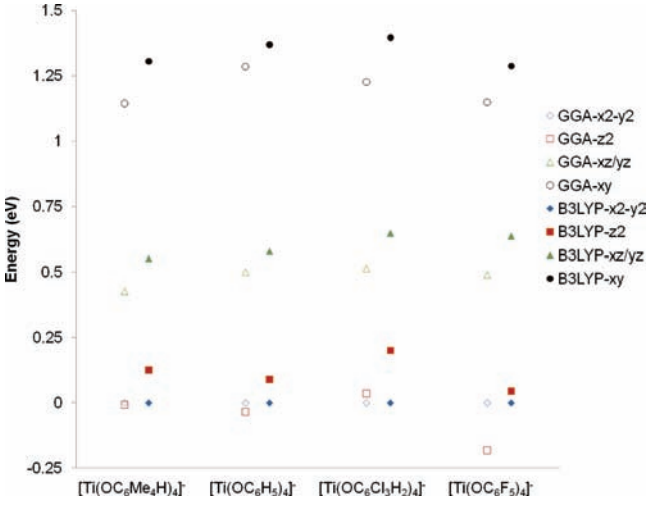

Figure 9. Relative d-orbital energies for the computed $[Ti(OAr)_4]$ species. For each species the results with both GGA-BP and hybrid B3LYP functional are shown.

by occupation with d electrons, but are also evident in the d^5 $[Fe(III)(OAr)_4]^-$ analogs. The energy separations between the d_{xy} and the $d_{xz/yz}$ orbitals and between the d_{z^2} and the $d_{x^2-y^2}$ orbitals depicted in Figures 9 and 10 and listed in Table 5 are less

dx.doi.org/10.1021/ic2003782 |Inorg. Chem. 2011, 50, 6584–6596

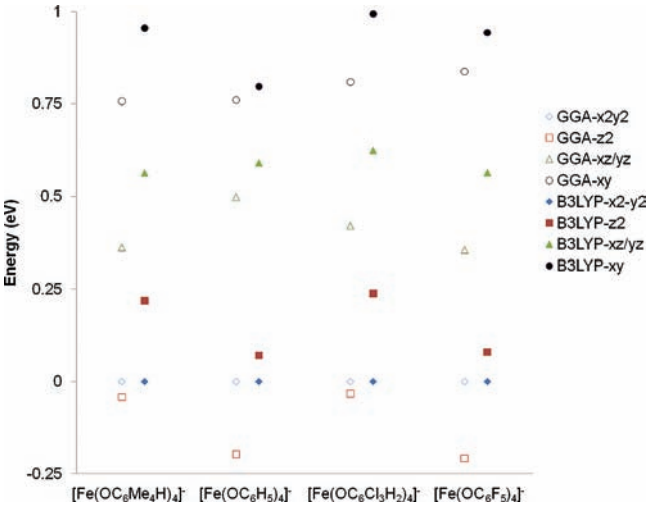

Figure 10. Relative d-orbital energies for the computed $[Fe(III)(OAr)_4]^-$ species. For each species the results with both GGA-BP and hybrid B3LYP functional are shown.

Table 5. Absolute Values of Energy Differences (eV) within Ligand Fields for $[Ti(IV)(OAr)_4]$ and $[Fe(III)(OAr)_4]^-$ Complexes

compound	functional	$\|\Delta E\|$ ($d_{xy} - d_{xz}/d_{yz}$)	$\|\Delta E\|$ ($d_{x^2-y^2} - d_{z^2}$)
$[Ti(OC_6Me_4H)_4]^-$	GGA-BP	0.7157	0.0077
	B3LYP	0.7542	0.1257
$[Ti(OC_6H_5)_4]^-$	GGA-BP	0.7844	0.0350
	B3LYP	0.7903	0.0894
$[Ti(OC_6Cl_3H_2)_4]^-$	GGA-BP	0.7108	0.3513
	B3LYP	0.7483	0.2005
$[Ti(OAr^F)_4]^-$	GGA-BP	0.6582	0.1820
	B3LYP	0.6512	0.0450
$[Fe(OC_6Me_4H)_4]^-$	GGA-BP	0.3956	0.0427
	B3LYP	0.3930	0.2190
$[Fe(OC_6H_5)_4]^-$	GGA-BP	0.2625	0.1977
	B3LYP	0.2077	0.0708
$[Fe(OC_6Cl_3H_2)_4]^-$	GGA-BP	0.3889	0.0327
	B3LYP	0.3700	0.2384
$[Fe(OAr^F)_4]^-$	GGA-BP	0.4824	0.2083
	B3LYP	0.3794	0.0796

strongly indicative of these differences but are still qualitatively consistent. In the absence of π donation, the d_{xy} orbital is expected to be raised less above the $d_{xz/yz}$ pair, as is clearly seen when comparing the end members of the series. Similarly, the d_{z^2} orbital is expected to be below the $d_{x^2-y^2}$ orbital in the absence of π donation but will be raised above as π donation increases. The d_{z^2} orbital is raised least in the perfluorophenolate case, although the $OC_6Cl_3H_2$ ligand is anomalously high in the B3LYP calculation.

In general, the GGA-BP and B3LYP calculations agree with one another, although with less consistency observed in the former *e* set than the former t_2 set of orbitals. The $OC_6Cl_3H_2$ ligand generally shows less π donation than the OC_6Me_4H ligand but not as much as was expected. We attribute this to the artificial D_{2d} constraint which forces the ortho substituents to be close to the O 2p orbital perpendicular to the phenolate plane. Rotation of the phenyl group would relieve this stereoelectronic clash but reduce the symmetry.

CONCLUSIONS

We prepared homoleptic Fe(II) and Fe(III) phenolate compounds with the $[Fe(OAr)_m]^{n-}$ motif by using highly fluorinated ligands that have reduced ligand π-donor character and prevent bridging without using steric bulk. The four mononuclear Fe(III) derivatives are pentacoordinate red-orange compounds and exhibit high-spin behavior in solution. The pale-yellow divalent $[Fe(OAr^F)_4]^{2-}$ compound is also high spin and has pseudotetrahedral geometry, which is very similar to the known $[Co(OAr^F)_4]^{2-}$ and $[Ni(OAr^F)_4]^{2-}$ species.[18,19] Treatment of compound **3a** with PhIO resulted in ligand loss and dimer formation by presumed ligand oxidation and phenoxyl radical dissociation. DFT calculations demonstrated that under D_{2d} symmetry π donation from the O 2p orbitals is primarily into the d_{xy} and d_{z^2} orbitals. The degree of donation is qualitatively consistent with expectations based on ligand Brønsted basicity and supports the contention that fluorinated phenolate ligands facilitate isolation of nonbridged homoleptic complexes due to their reduced π basicity at oxygen.

ASSOCIATED CONTENT

Supporting Information. Figures S1 and S2 are ORTEP diagrams for **3b** and **6** and CIF included files for all compounds. This material is available free of charge via the Internet at http://pubs.acs.org.

AUTHOR INFORMATION

Corresponding Author

*E-mail: doerrer@bu.edu.

Notes

[⊥]In memoriam, Professor Michelle Millar (1946−2011).

ACKNOWLEDGMENT

We thank Boston University, Barnard College, and the NSF for financial support (NSF CAREER 0134817 and NSF-CHE 0910647 to L.H.D., NSF-CHE 0619339 to Boston University for the purchase of an NMR spectrometer, and NSF-DUE-9952633 to Barnard College for the purchase of an NMR spectrometer).

REFERENCES

(1) Baker, E. N.; Andeson, B. F.; Baker, H. M.; Haridas, M.; Norris, G. E.; Rumball, S. V.; Smith, C. A. *Pure Appl. Chem.* **1990**, *62*, 1067–1070.

(2) Peterson, N. A.; Arcus, V. L.; Anderson, B. F.; Tweedie, J. W.; Jameson, G. B.; Baker, E. N. *Biochemistry* **2002**, *41*, 14167–14175.

(3) Gahan, L. R.; Smith, S. J.; Neves, A.; Schenk, G. *Eur. J. Inorg. Chem.* **2009**, *2009*, 2745–2758.

(4) Mitic, N.; Hadler, K. S.; Gahan, L. R.; Hengge, A. C.; Schenk, G. *J. Am. Chem. Soc.* **2010**, *132*, 7049–7054.

(5) Costas, M.; Mehn, M. P.; Jensen, M. P.; Que, L., Jr. *Chem. Rev.* **2004**, *104*, 939–986.

(6) Lange, S. J.; Que, L., Jr. *Curr. Opin. Chem. Biol.* **1998**, *2*, 159–172.

(7) Wallar, B. J.; Lipscomb, J. D. *Chem. Rev.* **1996**, *96*, 2625–2657.

(8) Henderson, K. W.; Mulvey, R. E.; Reinhard, F. B. M.; Clegg, W.; Horsburgh, L. *J. Am. Chem. Soc.* **1994**, *116*, 10777–10778.

(9) Boyle, T. J.; Pedrotty, D. M.; Alam, T. M.; Vick, S. C.; Rodriguez, M. A. *Inorg. Chem.* **2000**, *39*, 5133–5146.
(10) Churchill, M. R.; Ziller, J. W.; Freudenberger, J. H.; Schrock, R. R. *Organometallics* **1984**, *3*, 1554–1562.
(11) Rothwell, I. P. *Chem. Commun.* **1997**, *33*, 1331–1338.
(12) Darensbourg, D. J.; Wildeson, J. R.; Yarbrough, J. C.; Reibenspies, J. H. *J. Am. Chem. Soc.* **2000**, *122*, 12487–12496.
(13) Kim, E.; Chufan, E. E.; Kamaraj, K.; Karlin, K. D. *Chem. Rev.* **2004**, *104*, 1077–1133.
(14) Lewis, E. A.; Tolman, W. B. *Chem. Rev.* **2004**, *104*, 1047–1076.
(15) Mirica, L. M.; Ottenwaelder, X.; Stack, T. D. P. *Chem. Rev.* **2004**, *104*, 1013–1045.
(16) Bradley, D. C.; Mehrotra, R. C.; Rothwell, I. P.; Singh, A. *Alkoxo and Aryloxo Derivatives of Metals*; Academic Press: New York, 2001; p 704.
(17) Koch, S. A.; Millar, M. *J. Am. Chem. Soc.* **1982**, *104*, 5255–5257.
(18) Buzzeo, M. C.; Iqbal, A. H.; Long, C. M.; Millar, D.; Patel, S.; Pellow, M. A.; Saddoughi, S. A.; Smenton, A. L.; Turner, J. F. C.; Wadhawan, J. D.; Compton, R. G.; Golen, J. A.; Rheingold, A. L.; Doerrer, L. H. *Inorg. Chem.* **2004**, *43*, 7709–7725.
(19) Zheng, B. N.; Miranda, M. O.; DiPasquale, A. G.; Golen, J. A.; Rheingold, A. L.; Doerrer, L. H. *Inorg. Chem.* **2009**, *48*, 4274–4276.
(20) Childress, M. V.; Millar, D.; Alam, T. M.; Kreisel, K. A.; Yap, G. P. A.; Zakharov, L. N.; Golen, J. A.; Rheingold, A. L.; Doerrer, L. H. *Inorg. Chem.* **2006**, *45*, 3864–3877.
(21) Cantalupo, S. A.; Lum, J. S.; Buzzeo, M. C.; Moore, C.; DiPasquale, A. G.; Rheingold, A. L.; Doerrer, L. H. *Dalton Trans.* **2010**, *39*, 374–383.
(22) Sun, Y.; Metz, M. V.; Stern, C. L.; Marks, T. J. *Organometallics* **2000**, *19*, 1625–1627.
(23) Metz, M. V.; Sun, Y.; Stern, C. L.; Marks, T. J. *Organometallics* **2002**, *21*, 3691–3702.
(24) Allen, F. H. *Acta Crystallogr., Sect. B* **2002**, *B58*, 380–388.
(25) Teo, B. K.; Antonio, M. R.; Tieckelmann, R. H.; Silvis, H. C.; Averill, B. A. *J. Am. Chem. Soc.* **1982**, *104*, 6126–6129.
(26) Cleland, W. E.; Holtman, D. A.; Sabat, M.; Ibers, J. A.; DeFotis, G. C.; Averill, B. A. *J. Am. Chem. Soc.* **1983**, *105*, 6021–6031.
(27) Kanatzidis, M. G.; Baenziger, N. C.; Coucouvanis, D.; Simopoulos, A.; Kostikas, A. *J. Am. Chem. Soc.* **1984**, *106*, 4500–4511.
(28) Canada-Vilalta, C.; Pink, M.; Christou, G. *Chem. Commun.* **2003**, 1240–1241.
(29) Canada-Vilalta, C.; O'Brien, T. A.; Pink, M.; Davidson, E. R.; Christou, G. *Inorg. Chem.* **2003**, *42*, 7819–7829.
(30) Stamatatos, T. C.; Christou, A. G.; Mukherjee, S.; Poole, K. M.; Lampropoulos, C.; Abboud, K. A.; O'Brien, T. A.; Christou, G. *Inorg. Chem.* **2008**, *47*, 9021–9034.
(31) Kanamori, D.; Yamada, Y.; Onoda, A.; Okamura, T.-a.; Adachi, S.; Yamamoto, H.; Ueyama, N. *Inorg. Chim. Acta* **2005**, *358*, 331–338.
(32) Nasri, H.; Fischer, J.; Weiss, R.; Bill, E.; Trautwein, A. *J. Am. Chem. Soc.* **1987**, *109*, 2549–2550.
(33) Byrn, M. P.; Curtis, C. J.; Hsiou, Y.; Khan, S. I.; Sawin, P. A.; Tendick, S. K.; Terzis, A.; Strouse, C. E. *J. Am. Chem. Soc.* **1993**, *115*, 9480–9497.
(34) Hung, C.-H.; Chang, C.-H.; Ching, W.-M.; Chuang, C.-H. *Chem. Commun.* **2006**, 1866–1868.
(35) Tsai, M.-C.; Tsai, F.-T.; Lu, T.-T.; Tsai, M.-L.; Wei, Y.-C.; Hsu, I. J.; Lee, J.-F.; Liaw, W.-F. *Inorg. Chem.* **2009**, *48*, 9579–9591.
(36) Evans, D. F. *J. Chem. Soc.* **1959**, 2003–2005.
(37) Sur, S. K. *J. Magn. Reson.* **1989**, *82*, 169–173.
(38) Sheldrick, G. M. *Acta Crystallogr., Sect. A* **2008**, *A64*, 112–122.
(39) Armstrong, W. H.; Lippard, S. J. *Inorg. Chem.* **1985**, *24*, 981–982.
(40) Evans, P. J. M.; Fitzsimmons, B. W.; Marshall, W. G.; Golder, A. J.; Larkworthy, L. F.; Povey, D. C.; Smith, G. W. *J. Chem. Soc., Dalton Trans.* **1992**, 1065–1068.
(41) Giusti, M.; Solari, E.; Giannini, L.; Floriani, C.; Chiesi-Villa, A.; Rizzoli, C. *Organometallics* **1997**, *16*, 5610–5612.
(42) Addison, A. W.; Rao, T. N.; Reedijk, J.; Van, R. J.; Verschoor, G. C. *J. Chem. Soc., Dalton Trans.* **1984**, 1349–1356.
(43) Yang, L.; Powell, D. R.; Houser, R. P. *Dalton Trans.* **2007**, *36*, 955–964.
(44) Abraham, M. H.; Duce, P. P.; Morris, J. J.; Taylor, P. J. *J. Chem. Soc., Faraday Trans.* **1987**, *83*, 2867–2881.
(45) Cai, J.; Lu, J. *Chin. J. Struct. Chem.* **1988**, *7*, 57–60.
(46) Esposito, V.; Solari, E.; Floriani, C.; Re, N.; Rizzoli, C.; Chiesi-Villa, A. *Inorg. Chem.* **2000**, *39*, 2604–2613.
(47) McGuinness, D. S.; Marshall, E. L.; Gibson, V. C.; Steed, J. W. *J. Polym. Sci., Part A: Polym. Chem.* **2003**, *41*, 3798–3803.
(48) Chang, J.-C.; Ho, W.-Y.; Sun, I. W.; Chou, Y.-K.; Hsieh, H.-H.; Wu, T.-Y.; Liang, S.-S. *Polyhedron* **2010**, *29*, 2976–2984.
(49) Bartlett, R. A.; Ellison, J. J.; Power, P. P.; Shoner, S. C. *Inorg. Chem.* **1991**, *30*, 2888–2894.
(50) Coucouvanis, D.; Greiwe, K.; Salifoglou, A.; Challen, P.; Simopoulos, A.; Kostikas, A. *Inorg. Chem.* **1988**, *27*, 593–594.
(51) McElearney, J. N.; Merchant, S. *Inorg. Chem.* **1978**, *17*, 1207–1215.
(52) Dolling, B.; Gillon, A. L.; Orpen, A. G.; Starbuck, J.; Wang, X.-M. *Chem. Commun.* **2001**, *37*, 567–568.
(53) James, B. D.; Liesegang, J.; Bakalova, M.; Reiff, W. M.; Skelton, B. W.; White, A. H. *Inorg. Chem.* **1995**, *34*, 2054–2057.
(54) Feist, M.; Troyanov, S. I.; Mehner, H.; Witke, K.; Kemnitz, E. *Z. Anorg. Allg. Chem.* **1999**, *625*, 141–146.
(55) Zhang, X.-X.; Lippard, S. J. *Inorg. Chem.* **2000**, *39*, 4388–4389.
(56) Day, P.; Joergensen, C. K. *J. Chem. Soc., Suppl.* **1964**, 6226–6234.
(57) Advanced Chemistry Development Software, ACD/Labs, 1994—2011.